

This work was written as part of one of the author's official duties as an Employee of the United States Government and is therefore a work of the United States Government. In accordance with 17 U.S.C. 105, no copyright protection is available for such works under U.S. Law.

Public Domain Mark 1.0

<https://creativecommons.org/publicdomain/mark/1.0/>

Access to this work was provided by the University of Maryland, Baltimore County (UMBC) ScholarWorks@UMBC digital repository on the Maryland Shared Open Access (MD-SOAR) platform.

Please provide feedback

Please support the ScholarWorks@UMBC repository by emailing scholarworks-group@umbc.edu and telling us what having access to this work means to you and why it's important to you. Thank you.

PROCEEDINGS OF SPIE

[SPIDigitalLibrary.org/conference-proceedings-of-spie](https://spiedigitallibrary.org/conference-proceedings-of-spie)

Development of x-ray microcalorimeter imaging spectrometers for the X-ray Surveyor mission concept

Bandler, Simon, Adams, Joseph, Chervenak, James, Datesman, Aaron, Eckart, Megan, et al.

Simon R. Bandler, Joseph S. Adams, James A. Chervenak, Aaron M. Datesman, Megan E. Eckart, Fred M. Finkbeiner, Richard L. Kelley, Caroline A. Kilbourne, Gabriele Betancourt-Martinez, Antoine R. Miniussi, Frederick S. Porter, John E. Sadleir, Kazuhiro Sakai, Stephen J. Smith, Thomas R. Stevenson, Nicholas A. Wakeham, Edward J. Wassell, Wonsik Yoon, Dan Becker, Douglas Bennett, William B. Doriese, Joseph W. Fowler, Johnathan D. Gard, Gene C. Hilton, Benjamin Mates, Kelsey M. Morgan, Carl D. Reintsema, Daniel Swetz, Joel N. Ullom, Saptarshi Chaudhuri, Kent D. Irwin, Sang-Jun Lee, Alexey Vikhlinin, "Development of x-ray microcalorimeter imaging spectrometers for the X-ray Surveyor mission concept," Proc. SPIE 9905, Space Telescopes and Instrumentation 2016: Ultraviolet to Gamma Ray, 99050Q (19 July 2016); doi: 10.1117/12.2232156

SPIE.

Event: SPIE Astronomical Telescopes + Instrumentation, 2016, Edinburgh, United Kingdom

Development of x-ray microcalorimeter imaging spectrometers for the X-ray Surveyor mission concept

Simon R. Bandler^a, Joseph S. Adams^{a,b}, James A. Chervenak^a, Aaron M. Datesman^{a,g}, Megan E. Eckart^a, Fred M. Finkbeiner^{a,f}, Richard L. Kelley^a, Caroline A. Kilbourne^a, Gabriele Betancourt-Martinez^{a,c}, Antoine R. Miniussi^{a,d}, Frederick S. Porter^a, John E. Sadleir^a, Kazuhiro Sakai^{a,d}, Stephen J. Smith^{a,b}, Thomas R. Stevenson^a, Nicholas A. Wakeham^{a,e}, Edward J. Wassell^{a,g}, Wonsik Yoon^{a,e}, Dan Becker^h, Douglas Bennett^h, William B Doriese^h, Joseph W. Fowler^h, Johnathon D. Gard^{h,i}, Gene C. Hilton^h, Benjamin Mates^{h,i}, Kelsey M. Morgan^h, Carl D. Reintsema^h, Daniel Swetz^h, Joel N. Ullom^{h,i}, Saptarshi Chaudhuri^j, Kent D. Irwin^j, Sang-Jun Lee^j, and Alexey Vikhlinin^k

^aNASA - Goddard Space Flight Center, Greenbelt, MD 20771, USA

^bCRESST & University of Maryland Baltimore County, Baltimore, MD 21250, USA

^cCRESST & University of Maryland College Park, College Park, MD 20742, USA

^dCRESST & Universities Space Research Assoc., Greenbelt, MD 20771, USA

^eNASA Postdoctoral Program, Universities Space Research Assoc., Greenbelt, MD 20771, USA

^fWyle Information Systems Inc., McLean, VA 22102, USA

^gStinger-Ghaffarian Technologies, Greenbelt 20771, USA

^hNational Institute of Standards and Technology, Boulder, CO 80305, USA

ⁱColorado University, Boulder, CO 80309, USA

^jStanford University, Palo Alto, CA 94305, USA

^kSmithsonian Astrophysical Observatory, Cambridge, MA 02912, USA

ABSTRACT

Four astrophysics missions are currently being studied by NASA as candidate large missions to be chosen in the 2020 astrophysics decadal survey.¹ One of these missions is the “*X-Ray Surveyor*” (XRS), and possible configurations of this mission are currently under study by a science and technology definition team (STDT). One of the key instruments under study is an X-ray microcalorimeter, and the requirements for such an instrument are currently under discussion. In this paper we review some different detector options that exist for this instrument, and discuss what array formats might be possible. We have developed one design option that utilizes either transition-edge sensor (TES) or magnetically coupled calorimeters (MCC) in pixel array-sizes approaching 100 kilo-pixels. To reduce the number of sensors read out to a plausible scale, we have assumed detector geometries in which a thermal sensor such a TES or MCC can read out a sub-array of 20-25 individual 1” pixels. In this paper we describe the development status of these detectors, and also discuss the different options that exist for reading out the very large number of pixels.

Keywords: X-ray Surveyor, microcalorimeter, hydra, multiplexing

1. INTRODUCTION

While the driving science and key capabilities of the *X-ray Surveyor* (XRS) observatory are just beginning to be studied by the STDT, based upon previous studies of future X-ray mission concepts with similar scientific goals, a microcalorimeter instrument appears to be highly desirable.³ The generally stated goals of achieving

Further author information: (Send correspondence to S.R.B.)

S.R.B.: E-mail: Simon.R.Bandler@nasa.gov, Telephone: 1 301 286 1363

high throughput, high-spectral and high angular resolution X-ray imaging, and extending the focal plane to at least 5 arc-minutes is a major challenge. Taken at the most basic level of interpretation, a square array of 1 arc-second pixels over this field-of-view would correspond to a detector array consisting of 90,000 pixels, a far higher number of X-ray microcalorimeter pixels than has so far been developed. In order to fully sample the point spread function of a 1 arc-second optic over this field-of-view, the array would more ideally approach a mega-pixel in size.

If the focal length of the X-ray optic is 10 meters, the same as Chandra,² the previous very high resolution X-ray optic, then 1 arc-second pixels will correspond to pixel sizes of approximately 50 μm , and the field-of-view would extend over an area of 1.5 x 1.5 cm. If shorter focal lengths are considered then even smaller pixels would be required, and it would be unlikely that a microcalorimeter would be able to meet the desired performance. If longer focal lengths are considered, then the problem becomes one of very large pixel count and also limited energy resolution for certain types of detector options. An energy resolution of less than 5 eV [FWHM] for each pixel is generally considered desirable over the energy range of 0.2-12 keV, with as high resolution as possible generally being desirable within the array size constraints.³ However, it may be acceptable to sacrifice some energy resolution in order to meet the rather challenging pixel number requirements.

In this paper we review what detector technology options currently exist that have the potential to meet the XRS desired array size scale, while maintaining sufficient energy resolution to carry out the X-ray spectroscopic measurements envisioned. While transition-edge sensors (TESs) and metallic magnetic calorimeters (MMCs) will be the main detectors discussed, we will also consider the potential of other detector technology options such as microwave kinetic inductance detectors (MKIDs) and magnetic penetration thermometers (MPTs). We will also discuss the practicality of using multi-absorber devices to effectively increase the number of pixels being read out, the options that might exist for hybrid arrays, and the range of pixel sizes that might be achievable based upon recent development. In addition we discuss what multiplexed read-out options exist that might make the electronics read-out of so many pixels practical at a temperature typically less than 100 mK.

2. DETECTOR TECHNOLOGY OPTIONS

There are two basic categories of low temperature X-ray detectors: those that operate at thermal equilibrium, and those that are inherently non-equilibrium devices. The equilibrium devices are more typically called microcalorimeters and in these devices each X-ray produces a temperature rise proportional to E/C , where E is the energy deposited by the X-ray, and C is the heat capacity of the device. For these devices the energy resolution is determined by the accuracy with which a very sensitive thermistor can measure a temperature rise on a background of temperature fluctuations caused by the random transport of energy between a body with heat capacity C , and the temperature bath to which is connected by a thermal conductance G . This is what is commonly known as thermodynamic noise, which scales as $\sqrt{k_B T^2 C}$.⁴ For high energy resolution, low temperatures (< 0.1 K) are needed to minimize C and to minimize these fluctuations. Examples of leading sensor technologies for these equilibrium detectors are semiconducting thermistors,⁵ transition-edge sensors (TES),⁶ metallic magnetic calorimeters (MMC)⁷ and magnetic penetration thermometers (MPT).⁸ In non-equilibrium detectors, the energy deposited by an X-ray generally remains as quantized excitations in the detector, such as quasiparticles in superconductors, whose energy is far from thermal equilibrium ($E \gg k_B T$). For these detectors low temperatures are still required to avoid thermally generated excitations. Examples of non-equilibrium detectors are superconducting tunnel junctions (STJ),⁹ and microwave kinetic inductance detectors (MKID).^{10,11}

In 1984, Moseley et al.¹² calculated that a full width at half maximum (FWHM) energy resolution of 1 eV should be possible while measuring 6 keV X-rays for microcalorimeters. Since that time there has been excellent progress towards meeting this level of energy resolution using many different detector types, as shown in Fig. 1. As can be seen from this plot, it has generally been the equilibrium microcalorimeters that have achieved the best energy resolution, with two microcalorimeter technologies having achieved FWHM energy resolution of under 2 eV (TES & MMC), and two others less than 4 eV (MPTs and silicon). In order to achieve very high resolving powers ($R=E/\Delta E$), above 2000, if the sensor is thermally well coupled to the absorber, it is necessary that the pixels come into thermal equilibrium on a time-scale that is of the order of R times the decay time. If not, then the amount of energy lost through thermal conduction to the heat bath will vary depending on the location of the X-ray event leading to degradation of energy resolution. In rough numbers, if the decay time is

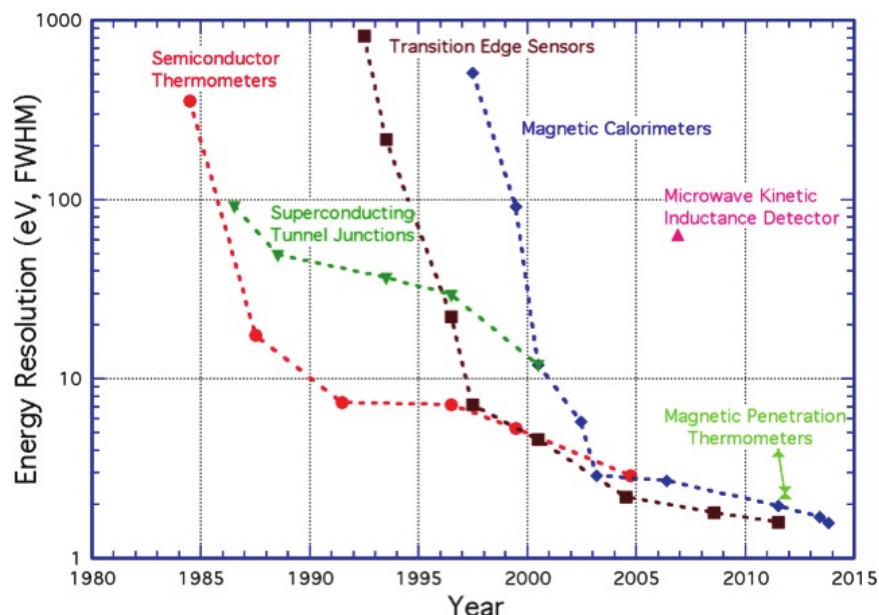


Figure 1. Approximate evolution of the best energy resolution while measuring 6 keV X-rays achieved for different detector technologies as a function of time.

0.5 ms, then the pixel should ideally come into thermal equilibrium on a time-scale faster than $0.25 \mu\text{s}$ to achieve an R of 2000. More exact criteria for the thermal conductance within the absorbers can be achieved through modeling.¹³ In cases where absorbers are known to take time to come into thermal equilibrium, if practical, it can be advantageous to introduce some thermal impedance in-between the sensor and the absorber.

While there is no fundamental reason why non-equilibrium devices could not achieve similar performance, in practice it has been difficult. To achieve the very high resolving powers of the equilibrium devices the non-equilibrium devices need to utilize very low energy excitations. This is necessary to avoid energy resolution degradation from statistical fluctuations in the number of excitations reaching the sensors. Typically not all the energy goes into non-equilibrium excitations; some goes into heat. Thus the number of the number of excitations sensed is governed by the statistics of excitation production and the statistical fluctuations on the division of energy. This requires the need for more excitations, and thus lower temperatures. For MKIDs and STJs, the energy of the quasi-particles is low enough that this condition is met. However a second condition to achieve very high R is that the number of excitations reaching the sensors is only dependent on the energy of the X-ray and not the location where the X-ray is absorbed. Experimentally it has been found in many non-equilibrium devices that the number can strongly depend on the 3-dimensional geometry of the devices, and whether there exist locations where the excitations can be trapped, even temporarily, leading to a non-uniform response depending on the location of the energy deposition. While this is not a major problem for bolometric applications or applications where relatively low R's are needed, this is a key issue for high-resolution X-ray spectroscopy, and is the likely reason why historically non-equilibrium devices have performed less well than equilibrium devices for X-ray spectroscopy. We note that recently an equilibrium version of the MKID has been under development.¹⁴ This approach has not yet achieved any better performance than non-equilibrium MKIDs.

TESs are typically operated by using joule heating to bias a superconducting thin metal film in-between its superconducting and normal metal states, where any small change in temperature produces a relatively large change in resistance. The TESs are usually attached to fast-thermalizing X-ray absorbers. These devices are voltage biased so that any change in resistance produces a change in current sensed using an extremely sensitive superconducting quantum interference device (SQUID) in an ammeter circuit.⁶ They are usually operated in a region of the transition where the change in resistance is approximately linearly dependent on temperature. However, since the bias circuit is voltage-biased, there will be some non-linearity in the response. Thus there will be some curvature in this "gain" curve that needs to be calibrated. The quasi-linear energy range of the

TES microcalorimeters, in which the gain curvature is relatively small, is determined by the heat capacity of the device as well as the steepness of the phase transition. While the design of TES X-ray microcalorimeters often relies on optimizing the absorber heat capacity (C) and quantum efficiency to achieve a high degree of linearity, alternative approaches exist with potential for even higher energy resolution using low- C absorbers, and letting the response be very non-linear.¹⁵ However, the difficulties associated with the use of very low heat capacity absorbers, the calibration of pixels, and other details of the implementation have meant that this kind of approach has historically not been popular.

One key advantage of TESs is that the resistance is typically highly temperature sensitive, leading to signals that are well above the read-out amplifier noise. This makes them relatively easy to read out in a multiplexed way in comparison with other sensor technologies. We will return to the read-out in Section 5. A second key advantage is that the X-ray microcalorimeter arrays are typically fabricated using standard lithographic microfabrication techniques, allowing the relatively straightforward fabrication of very large-format arrays. A significant disadvantage is the relative complexity of operating right in the middle of a phase transition, where the physics is very complicated,¹⁶ and the consequence that the properties of sensors are very sensitive to the magnetic field and to the TES superconducting transition temperature (T_c). The TES is usually a bilayer where T_c is controlled through the relative thicknesses of two metal films, one being a superconductor and the other a normal metal that proximitizes the superconductor, reducing T_c . The magnetic field seen by the TESs will depend on the ambient magnetic field, the self field of the current flowing within the TESs, and the current flowing in leads around the TESs. These all need to be kept extremely uniform for very large format uniform performance.

Two other very successful types of equilibrium microcalorimeter sensor technologies are semi-conducting thermistors and metallic magnetic calorimeters (MMCs). Both of these rely on equilibrium thermodynamics for their operation, and their performance is determined by conventional thermal transport physics. In particular, the performance of MMCs can be calculated from fundamental equilibrium thermodynamics.⁷ Excellent spectral performance has been achieved by both of these technologies: a FWHM of 3.2 eV at 6 keV for silicon,¹⁷ and 1.6 eV at 6 keV for MMCs.¹⁸ The main disadvantages of silicon thermistors is that no multiplexed read-out technology has been developed that is capable of matching those available to TESs, MKIDs etc. (see Section 5). Multiplexing of silicon thermistors is being developed by one group,¹⁹ however it currently utilizes an approach that generates a lot of power at low temperatures, and thus might not be practical for extremely large-format arrays. In addition, the devices are traditionally fabricated using steps involving hand-assembly of the arrays, making them very hard to produce in large format arrays. The full microfabrication of silicon thermistor arrays with absorbers integrated has not yet been demonstrated.

MMCs utilize the temperature dependence of paramagnets, where the magnetization is proportional to $1/T$. The change in magnetization produces a change in flux coupled to a SQUID magnetometer. This sensor technology has a number of advantages over the other technologies. As well as relying on calculable equilibrium thermodynamics to determine the performance, this sensor has the advantage that no heat is dissipated in reading out the sensor. This makes the thermal design of very large arrays much simpler and also means that there is no Johnson noise to limit the performance, and is therefore only limited by phonon noise and the noise associated with the SQUID read-out. The removal of Johnson noise means that in principle better energy resolution can be achieved with MMCs than with, for instance TESs. However, because the energy resolution is limited by SQUID noise, unlike TESs, the energy resolution is typically very sensitive to the achievable SQUID noise. When multiplexed with an MMC version of time-division multiplexing,²⁰ then the achievable energy resolution of an MMC degrades significantly from the single pixel performance unless a very advanced SQUID read-out design is produced. However, when considering microwave SQUID read-out options (considered later), this is much less of a problem, and degradation of energy resolution should be avoidable.

In comparison with TESs, MMCs have a relatively poor sensitivity to temperature, the relative change in magnetization as a function of temperature ($\frac{T}{M} \frac{\partial M}{\partial T}$) = -1. For this reason, as well as the lack of Johnson noise, the optimization of the coupling efficiency of MMCs to SQUIDs is critical. Interestingly MMCs and TESs end up having very similar dependence of X-ray event size to bath temperature. While MMC signal sizes are much less sensitive to the heat bath temperature, TESs make up for being more sensitive by self-heating well above

the bath temperature to the transition temperature, where fluctuations of bath temperature then have much less of an effect on the TES temperature.

A variation on MMCs and TESs that uses some advantages of both technologies are magnetic penetration thermometers (MPTs). These utilize the relatively large change in the diamagnetism of a superconductor as it goes through the phase transition from superconducting to normal.⁸ MPTs are similar to MMCs in the way the signals are coupled from thin films to the SQUID read-out without requiring joule heating and the associated Johnson noise. In addition, they have the relatively high temperature sensitivity of phase transitions of TESs, boosting the responsivity of signals and making the signals much larger than the SQUID noise. Indeed, a FWHM energy resolution of under 2 eV has been achieved in an MPT array with close-packed AuBi absorbers, and a FWHM of 2.3 eV at 6 keV.⁸ While this technology has a lot of potential for excellent energy resolution, it does have the same disadvantage as TESs of operating in complicated phase transitions and being very sensitive to magnetic fields, without some of the advantages of TESs such as being as easy to be read out without very optimized coupling circuits. These devices also have a responsivity to energy that is far more sensitive to heat bath temperature fluctuation than TESs or MMCs.

3. PIXEL SIZE

As described in Section 1, one of the most important parameters in the design of X-ray microcalorimeter arrays for the X-ray Surveyor is the small size and detection efficiency of close-packed pixels in arrays of microcalorimeters. While Hitomi²¹ used square pixels around 850 μm in size, and Athena²² is considering the use of 250-300 μm pixel sizes,²³ XRS requires much smaller pixel sizes. If the focal length of the X-ray optic is 10 meters then pixel sizes that correspond to 1" are 50 μm . If longer focal lengths are considered, such as 20 meters, then this pixel size will correspond to 0.5". This pixel size is close to the smallest that has previously been achieved in small TES X-ray microcalorimeters developed for Solar and X-ray astrophysics.^{24,25}

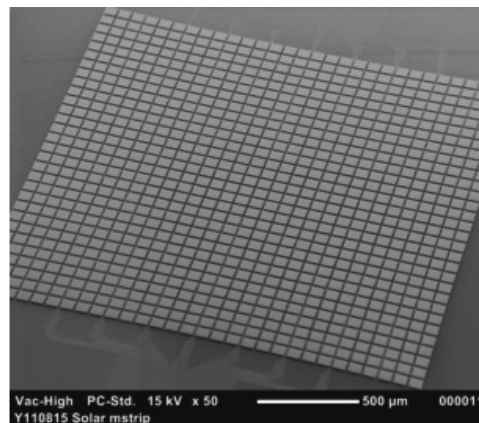


Figure 2. Scanning electron microscope image of a close-packed 32×32 array of microcalorimeter pixels on a 75 μm pitch.

Small TES microcalorimeters developed so far have all been designed with the superconducting bilayers deposited directly onto a solid substrate rather than the more traditional approach of depositing them on silicon nitride membranes.²⁶ The use of silicon nitride membranes was introduced for two reasons. First it enabled the mechanical construction of a relatively weak thermal link between the TES and the heat bath, determined by the membrane thickness and temperature of operation. Second, this membrane ensured that a significant number of non-equilibrium phonons produced immediately after the X-ray energy is deposited, but before coming into thermal equilibrium,²⁷ could not escape. This athermal phonon loss is minimized because the geometry of the membrane is such that very few can enter into it before thermal equilibrium is reached. For pixels on a very fine pitch, there is very little space for running out the wires underneath the over-hanging absorbers, in-between the TESs. It is almost impossible to imagine fabricating them with individual membranes around each pixel

and with well heat-sunk regions around the pixels as well, as would be necessary to build a large array. Good heat-sinking to each pixel is essential to maintain a common bath temperature for each pixel, and thus uniform array performance, and also to minimize thermal cross-talk between pixels.

With the TES deposited on a solid substrate like silicon the thermal conductance (G) to the heat bath is determined purely by the thermal boundary resistance of phonons to the heat bath. Excellent heat-sinking within the silicon substrate can be achieved through use of a buried copper layer.²⁸ This thermal conductance path is typically much stronger than in silicon nitride membranes, but is determined by the area of contact and temperature of operation. The temperature dependence is relatively strong, with G varying as T^3 . Therefore the TES temperature of operation strongly affects not just the energy resolution and energy range for detecting X-rays, but also the thermal time constant, and therefore the associated count rate capability of the microcalorimeter and the ease of multiplexing. Athermal phonon loss is minimized through the minimization of the area on contact between the TESs and the X-ray absorbers that are cantilevered above the TES film.²⁹

Excellent energy resolution has been achieved in small TES X-ray microcalorimeters fabricated on solid silicon substrates. The best energy resolution achieved in any X-ray microcalorimeter at 6 keV was achieved in a pixel with a $57\mu\text{m}$ absorber, demonstrating a FWHM of 1.58 eV at 6 keV.²⁹ This device had a relatively high superconducting transition temperature (~ 90 mK at the operating bias) with an X-ray signal decay time of $200\mu\text{s}$, and was thus able to accommodate relatively high count rates of above 100 counts per second without significant energy resolution degradation. A much lower T_c small-pixel TES has demonstrated the best energy resolution of any X-ray microcalorimeter at lower energies, with a FWHM of 0.70 eV demonstrated at 1.5 keV²⁵ for a pixel $45\mu\text{m}$ in size, in an array with a $50\mu\text{m}$ pitch. At lower energies (<1 keV), energy resolution as good as 0.5 eV was possible, and the decay time for the X-ray pulses was 1.2 ms.

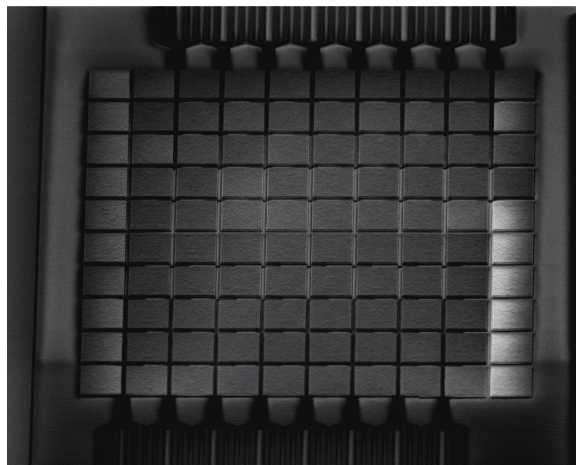


Figure 3. Scanning electron microscope image of a 10×10 array of pixels on a $25\mu\text{m}$ pitch.

A scanning electron microscope image of a 32×32 arrays of pixels on a $75\mu\text{m}$ pitch, fully wired with microstrip, is shown in Fig. 2. A key aspect to the development of compact arrays is the routing of wires. In general, for an $N \times N$ array of any microcalorimeter, where the wiring comes out in the same plane as the sensors in between pixels, there are a maximum of $N/4$ wire-pairs in gaps between sensors. Therefore the most efficient routing of a 32×32 array requires a maximum of 8 pairs of wires between any two pixels. The pitch of the microstrip wiring here was $4\mu\text{m}$, with the lower lead width being $2.5\mu\text{m}$, the upper layer width being $1.5\mu\text{m}$, and the gap between adjacent microstrips being $1.5\mu\text{m}$. The critical current of this wiring was greater than 1 mA, more than sufficient for carrying the TES current.

In a recent development as part of an on-going NASA research program, even finer pitch pixels and associated wiring are being developed. Fig. 3 shows scanning electron microscope and photographic images of an array of pixels on a $25\mu\text{m}$ pitch. The TESs underneath that are $\sim 7\mu\text{m}$ in size. The microstrip wire pairs have a pitch

of $2\ \mu\text{m}$ for these devices, and have already been shown to have sufficiently high critical current for reading out the TESs. These new devices are still undergoing development, and have shown transition shapes as expected.¹⁶

4. HYDRAS

For large arrays of small-pixels, such as is needed by the X-ray Surveyor, the use of “hydras” is the ideal approach. A “hydra” is a position-sensitive microcalorimeter that consists of multiple absorbers coupled to a single readout sensor each with a different thermal conductance,^{30,31} as depicted in Fig. 4(a). This type of geometry allows an increase the number of pixels relative to the number of readout channels. The basic idea is that the sensor will measure a different characteristic signal depending upon which pixel has absorbed the incident photon. After the initial position-dependent equilibration signal, the pulses decay with the same exponential rate. Position information is determined from the pre-equilibration signal, which can be measured using a simple rise-time measurement or, if increased sensitivity is required (typically at lower energies), more complicated signal processing algorithms may be implemented. The photon energy is then calculated using a single digital optimal filter referenced for each absorber element. Hydras can be made using any thermal sensor, and have been demonstrated with both TES and MMC sensors. Fig. 4(a) shows a simple thermal model of a 4-pixel hydra coupled to a single readout sensor and the time evolution of the measured signals and a scanning electron microscope image of a 9-absorber Hydra is shown in Fig. 4(b).

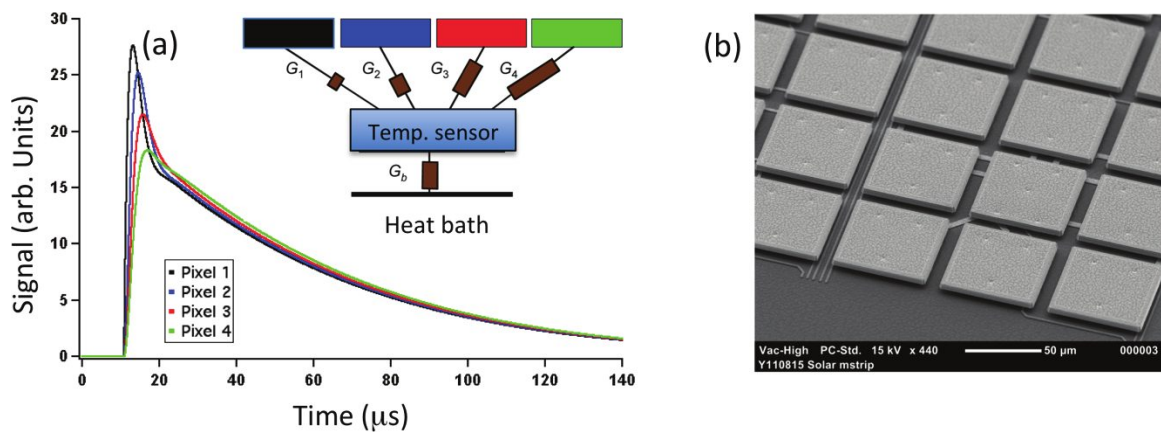


Figure 4. (a) Time evolution of pulse shape corresponding to photon absorption in each of the 4 absorbers. Position discrimination between the absorbers is achieved using the pre-equilibration signal. Inset is the thermal model of the 4-pixel hydra concept, consisting of 4 absorbers each with a different thermal conductance link to the sensor. (c) Photograph of a 9-absorber TES hydra.

To first order, the energy resolution of individual microcalorimeters scales as the square root of heat capacity. For a hydra with an $n \times n$ array of absorbers attached, the FWHM energy resolution therefore should scale as n due to the increased heat capacity and with it thermodynamic noise due to energy fluctuations between the hydra and the heat bath.⁵ In addition, there can be increased broad band noise associated with internal thermal fluctuations between the different absorbers and the sensor. This has been calculated for a number of different cases.³¹ However, if designed carefully, the internal thermal fluctuations do not degrade the energy resolution significantly, and is typically less than 25%. The use of hydras can also be considered as a way to achieve greater position sensitivity for a given sensor and net absorber size, essentially by partitioning the macro-absorber in a way that allows us to determine the location of the an X-ray event through the pulse-shape. In the hydra geometry, the count rate capability per pixel is not very high since so many pixels (absorbers) are attached to each sensor. However, the science goals of the X-ray surveyor are focused around observations of faint point sources and spatially extended X-ray sources. Because of this, a count rate capability of 5×5 hydras of approximately 20 counts per second could well be fully adequate for this mission’s observations.

In recent years, most hydras developed have used TESs as the sensors, many of them with very small absorbers attached allowing the pixel to maintain extremely good energy resolution. Two types of small-absorber hydras

have been developed, one with four absorbers attached to a single sensor, and one with 9 absorbers attached. The 9-absorber hydra is shown as an SEM image in Fig. 4(b). These have been extensively tested and have provided impressive energy resolution.³² The 4-absorber hydra has demonstrated an RMS FWHM energy resolution over 4 pixels of 1.4 eV at 1.5 keV and 2.0 eV at 6 keV. The 9-absorber hydra demonstrated an RMS FWHM energy resolution of 2.2 eV at 1.5 keV, and of 2.5 eV at 6 keV.

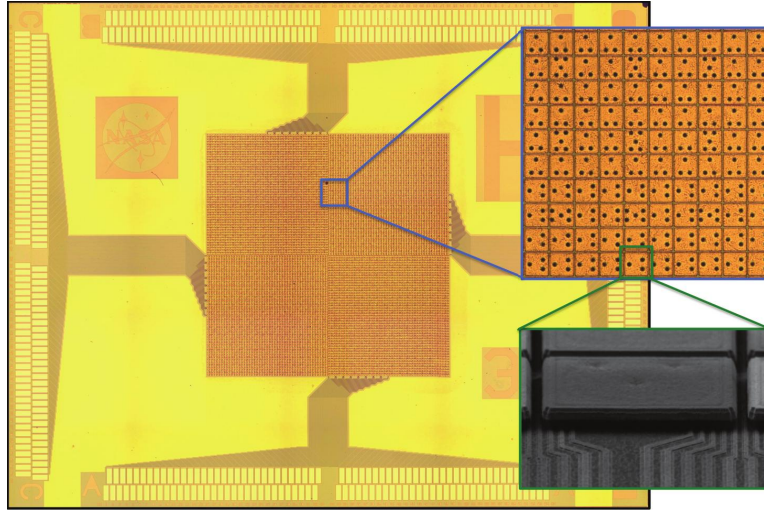


Figure 5. Photographic images of a 9.2 kilo-pixel array, based upon an array of 1024 TES sensors. Inset is first a photograph of a 10x10 region of the array, and then a scanning electron microscope image of one absorber. While all pixels are fully wired within the array, only a quarter of the TESs fan out to wire-bond pads around the perimeter of the array.

Fig. 5 illustrates how the use of this type of hydra can rapidly increase the number of microcalorimeter pixels in an array, without increasing the complexity of the focal plane assembly or the electronics read-out. It shows a 96x96 array (9216 pixels), fully wired within the array, with absorbers on a 75 μm pitch. This array is designed around a 32x32 grid of close-packed 3x3 TES-hydras. The gap between absorbers is 4 μm in this array, providing a 90% area filling factor. This hydra concept has the potential to be developed to have even more absorbers attached to each sensor. We have modeled the performance of hydras with 20 pixels attached and are currently developing this type of device. We have speculated that hydras with up to 25 absorbers should be possible, depending upon the size, speed and energy resolution requirements of the pixels.

5. READ-OUT DEVELOPMENT & LARGER ARRAYS

Perhaps the most significant factor that will determine the greatest number of pixels that can be accommodated in XRS arrays is the multiplexer read-out technology. TESs and MMCs are read out using superconducting-quantum-interference devices (SQUIDs). A typical read-out scheme employs a single SQUID (SQ1) in close proximity to the TES or MMC. An additional amplifier containing ~ 16 –100 SQUIDs in series then amplifies the signal to a level that can be handled by room-temperature electronics. If a full amplifier channel were provided for each detector in the array, the heat load from both the large number of SQUID series arrays and the large number of wires running to the TES cold bath would be prohibitive. At NIST a number of SQUID multiplexing architectures to read out large arrays of TESs have been developed, that we do not describe in detail here, but refer you to the large body of literature available.^{33–36}

In Fig. 6 we see a “*Moore’s Law*” plot of the largest number of TES pixels in arrays as a function of time, with all pixels in the array read out. The blue points and line represent the evolution of the largest array size fully read out in the past. The red line is a speculative extrapolation into the future. While kilo-pixel arrays are being tested, they do not show as a data point yet, since a system has not yet been built where all pixels have been read out. The doubling time until the present is approximately 2 years, which we have extrapolated forward until a

mega-pixel array size is achieved. The extrapolation curve is not necessarily meant to be predictive, but rather to provide some context for the likely timescale over which one might expect larger microcalorimeter arrays to become available. In particular, it suggests that 100 kilo-pixel arrays are conceivable for the later part of the 2020s decade, and a mega-pixel maybe achievable in the 2030s. There are many different factors that affect this evolution, the trade-offs of pixel number with energy resolution and detector speed being two of the most significant. While it is quite possible that this line could start to curve down going forward, the introduction of large-format hydra arrays and new approaches to read-out does provide some optimism that 100-kilo-pixel arrays and even mega-pixel microcalorimeter arrays could be possible on the time-scale implied by this plot.

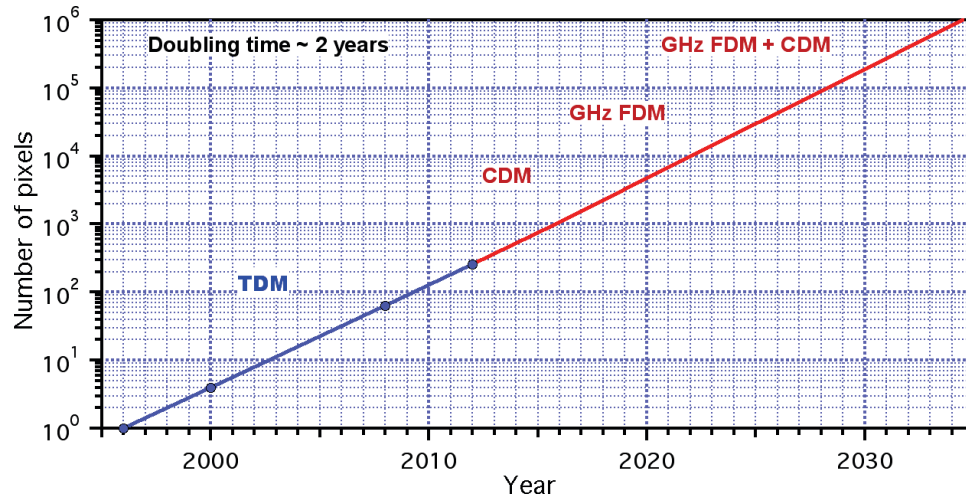


Figure 6. “Moore’s law” plot for the evolution of maximum arrays size as a function of time for reading out X-ray and γ -ray microcalorimeter arrays. The blue points represent past demonstrations, and the red line an extrapolation onto the future.

The different multiplexing technologies that roughly correspond to the different pixel number scales are labeled on the plot. As the number of pixels in arrays increases, the multiplexing technology will evolve. Starting with time-division multiplexing (TDM),³³ then evolving to code-division multiplexing (CDM),³⁴ then to multiplexing in the GHz frequency range with frequency domain multiplexing (GHz FDM), and finally to a combination of GHz FDM and CDM. There are other alternatives, and there will be overlaps in pixel number ranges over which these different technologies will be applicable, but they naturally build upon knowledge learned in previous read-out generations in their evolution.

Currently, the most mature technology for reading out X-ray microcalorimeters is time-division multiplexing, with several systems using this read-out worldwide.³⁸ TDM involves the sequential and cyclical read-out of SQUIDs each connected to TESs. Switches are used to sequentially switch on and off each SQUID in turn. TDM has recently been used to demonstrate the read-out 32-row TDM in a single read-out chain for TESs, with very little energy resolution degradation.³⁷ An average FWHM energy resolution of 2.55 eV was achieved from 30 TESs (two of the TDM SQUIDs had broken wire-bonds to the input and so did not have a TES attached). The average energy resolution when reading out each pixel individually was 2.40 eV, so the resolution degradation from multiplexing was minimal. We are currently developing a version of the electronics that is space flight compatible.

TDM, in its present form, is very close to meeting the required specifications for reading out the X-ray Surveyor microcalorimeter array. Using standard 32-row multiplexing of TESs, each of which is designed to be a 25-absorber hydra, then in principle the notional minimum acceptable number of pixels of 90,000 could be achieved with just 3600 TESs, and ~ 120 read-out chains. This number is similar to the expected number of read-out chains that is currently being baselined for the X-ray Integral Field Unit instrument (X-IFU) on ESA’s Athena mission. The X-IFU currently has a baseline of 3840 TESs, read out by 96 channels of FDM read-out, with each channel reading out 40 pixels.³⁹

A newer approach with the potential to read out even larger arrays uses a microwave SQUID multiplexer.³⁵ This approach uses unshunted rf SQUIDs coupled to superconducting microwave resonators. The resonators are spaced closely in frequency space, in principle allowing hundreds of resonators to be read out with each amplifier chain. This device provides hundreds of MHz up to several GHz of bandwidth with power dissipation less than 10 pW per pixel. Prototypes have shown high Q (5,000 - 20,000) and low flux noise ($0.17 \mu\Phi_0/\sqrt{\text{Hz}}$). The microwave SQUIDs can be used to read out TESs or magnetic calorimeters,⁴⁰ their optimization being slightly different for the two types of sensor. Each microwave SQUID channel could potentially be able to read out between hundreds to a few thousand TESs or magnetic calorimeters using two coaxial cables and a handful of low-frequency twisted pairs. If this potential is realized, then microwave SQUID read-out could provide a simpler scheme than TDM for reading out array sizes in the the range of 100 thousand to a million pixels.

To optimize MCC performance, we need a design that minimizes the SQUID coupled energy sensitivity (ϵ_s), and that maximizes the ratio of signal energy in the SQUID amplifier to that in the MCC sensor. A key aspect to this in large format arrays is that stray inductance from routing the wires can become large compared with the meander inductance and SQUID input inductance, causing poor matching of the meander inductance to the SQUID. To meet the desired optimal coupling we therefore need to increase the size of the meander inductance without increasing its area. Therefore the widths of lines and spaces in the pick-up coil meanders need to be reduced. This can best be done if we reduce the pitch of the meander from $5 \mu\text{m}$ to $0.8 \mu\text{m}$, with the Nb traces and the gaps in-between them both being reduced to $0.4 \mu\text{m}$ wide. Our group is currently investigating this approach.

In order to meet the minimum requirements of the X-ray Surveyor, a 300×300 array of pixels on a $50 \mu\text{m}$ pitch is required. Our group has tentative designs that meet these requirements with both TES and MMC sensors. These designs utilize hydras, of a larger pixel/absorber count than previously demonstrated and which will maintain better than ~ 4 eV resolution per pixel/absorber while still providing pixel/absorber discrimination for incident X-rays with energies down to 200 eV. We have calculated the estimated energy resolution, assuming an optimally designed SQUID for MMCs, given plausible estimates for the performance of fine-pitch meander pick-up coils, and for the stray inductance in a full-scale array. The estimated FWHM energy resolution is < 4.0 eV and the potential remains for resolutions of pixels in 5×5 hydras of < 3 eV.

6. CONCLUSIONS

Based upon the ongoing development of X-ray microcalorimeter arrays and their read-out, it is realistic to consider microcalorimeter array scales as desired by the X-ray Surveyor in the next decade. To reduce the number of sensors read out to a plausible scale for the X-ray Surveyor, the most promising detector geometries are those in which a thermal sensor such a TES or MCC can read out a sub-array of 20-25 individual $1''$ pixels. Position discrimination is achieved through the different pulse shapes produced, since each absorber is connected by a different strength thermal connection. If this scale of “hydra” design is successful, then the number of sensors that are needed to be read out is practical using TDM (~ 3600). Alternative read-out approaches also exist that utilize dissipationless microwave SQUIDs coupled to each sensor in resonator circuits in the GHz frequency range. This technology has not yet reached the same level of technical maturity. However, if successfully developed, this read-out has the potential for meeting and even exceeding the straw man read-out requirements with just a handful of signal chains.

REFERENCES

- [1] “Physics of the Cosmos Program Analysis Group (PhysPAG) Report on Flagship Mission Concepts to Study for the 2020 Decadal Survey”, James J. Bock et al., Physics of the Cosmos Executive Committee report, 8 October, 2015.
- [2] https://en.wikipedia.org/wiki/Chandra_X-ray_Observatory.
- [3] “SMART-X, Square meter arcsecond resolution x-ray telescope”, A. Vikhlinin, <http://pcos.gsfc.nasa.gov/studies/rfi/Vikhlinin-Alexey-RFI.pdf>
- [4] “Thermal Equilibrium Calorimeters An Introduction”, D. McCammon, in Cryogenic Particle Detection, 2005, vol. 99 of Topics in Applied Physics, ed. by C. Enss, pp. 1–34.

- [5] “Silicon Thermistors”, D. McCammon, in *Cryogenic Particle Detection*, 2005, vol. 99 of *Topics in Applied Physics*, ed. by C. Enss, pp. 35–61.
- [6] “Transition-Edge Sensors”, K.D. Irwin and G.C. Hilton in “*Topics in Applied Physics*”, Vol 99, pp. 63-149, 2005.
- [7] “Metallic magnetic calorimeters”, A. Fleischmann, C. Enss, and G.M. Seidel, in *Cryogenic Particle Detection*, 2005, vol. 99 of *Topics in Applied Physics*, ed. by C. Enss, pp. 151–216.
- [8] “Magnetically Coupled Microcalorimeters”, S.R. Bandler, K.D. Irwin, D. Kelly et al., *Journal of Low Temperature Physics* Volume: 167 Issue: 3-4 Pages: 254-268 (2012).
- [9] “Quantum Giaever Detectors”, P. Lerch, A. Zehnder, in *Cryogenic Particle Detection*, 2005, vol. 99 of *Topics in Applied Physics*, ed. by C. Enss, pp. 217–257.
- [10] “A superconducting detector suitable for use in large arrays”, P.K. Day, H.G. Leduc, B.A. Mazin, A. Vayonakis, and J. Zmuidzinas, *Nature*, 425:817821 (2003).
- [11] “A superconducting focal plane array for ultraviolet, optical, and near-infrared astrophysics”, B.A. Mazin, B. Bumble, S.R. Meeker, K. OBrien, S. McHugh, E. Langman, *Optics Express*, 20(2):15031511 (2012).
- [12] S.H. Moseley, J.C. Mather, D. McCammon, *J. Appl. Phys.* 56, 1257 (1984).
- [13] “Determining the thermal diffusivity in microcalorimeter absorbers and its effect on detector response”, T. Saab et al., *Journ. of Appl. Phys.* 102, 104502 (2007).
- [14] “Highly multiplexible thermal kinetic inductance detectors for x-ray imaging spectroscopy”, G. Ulbricht, B.A. Mazin, P. Szypryt, A.B. Walter, C. Bockstiegel, B. Bumble, *View ResearcherID and ORCID App. Phys. Lett.* Vol. 106 (25) 251103 (2015).
- [15] “Optimal Energy Measurement in Nonlinear Systems - An Application of Differential Geometry”, *Journ. of Low Temp. Phys.*, 176 (1-2), 6-26, (2014).
- [16] “Longitudinal Proximity Effects in Superconducting Transition-Edge Sensors”, J.E. Sadleir et al., *Phys. Rev. Lett.* 104, 047003 (2010).
- [17] “High resolution X-ray microcalorimeters”, F.S. Porter, R.L. Kelley, C.A. Kilbourne, *Nucl. Inst. & Methods in Phys. Res.A* 559 436-438 (2006).
- [18] “Direct-current superconducting quantum interference devices for the readout of metallic magnetic calorimeters”, S. Kempf, A. Ferring, A. Fleischmann, C. Enss *Superconductor Science and Technology*, Volume 28, Number 4 (2015).
- [19] “Toward large μ -calorimeters X-ray matrices based on Metal-Insulator sensors and HEMTs/SiGe Cryo-Electronics”, J.L. Sauvageot, C. Pigot, X. de la Broise, T. Charvolin, H. Sahin, M. Rodriguez, F. Lugiez, A. Le Coguie, Q. Dong, Y. JinJean-Luc. These proceedings.
- [20] “Time Domain Multiplexed Readout of Magnetically Coupled Calorimeters”, J.P. Porst, S.R. Bandler, J.S. Adams, et al., *Ieee Transactions on Applied Superconductivity* Volume: 23 Issue: 3 Published: (2013).
- [21] “The quiescent intracluster medium in the core of the Perseus cluster”, Aharonian et al., *Nature* 535, 4041 (2016).
- [22] “The Hot and Energetic Universe: A White Paper presenting the science theme motivating the Athena+ mission”, Nandra, K., Barret, D., Barcons, X., Fabian, A., den Herder, J.-W., Piro, L., Watson, M., Adami, C., Aird, J., Afonso, J. M., and et al., *ArXiv e-prints* (June 2013).
- [23] “TES pixel parameter design of the microcalorimeter array for the X-ray Integral Field Unit on Athena”, S.J. Smith et al., these proceedings.
- [24] “High Spectral Resolution, High Cadence, Imaging X-ray Microcalorimeters for Solar Physics”, S.R. Bandler et al., *Space Telescopes and Instrumentation 2010: 7732* (2010).
- [25] S.-J. Lee et al., *Appl. Phys. Lett.* 107, 223503 (2015).
- [26] “Uniform high spectral resolution demonstrated in arrays of TES x-ray microcalorimeters”, C.A. Kilbourne et al., *UV, X-ray, AND Gamma-ray Space Instrumentation for Astronomy XV* Volume: 6686 Pages: 68606 (2007).
- [27] “Athermal energy loss from x-rays deposited in thin superconducting films on solid substrates”, A.G. Kozorezov, C.J. Lambert, S.R. Bandler, et al., *Phys. Rev. B* 87, 104504 (2013).

- [28] “Development of embedded heatsinking layers for compact arrays of X-ray TES microcalorimeters”, F.M. Finkbeiner, C. N. Bailey, S. R. Bandler, R. P. Brekosky, A. D. Brown, J. A. Chervenak, M. E. Eckart, R. L. Kelley, D. P. Kelly, C. A. Kilbourne, F. S. Porter, J. E. Sadleir, and S. J. Smith, *IEEE Trans. Appl. Supercond.*, vol. 21, no. 3, pp. 223226, (2011).
- [29] “Small Pitch Transition-Edge Sensors with Broadband High Spectral Resolution for Solar Physics”, S.J. Smith, J.S. Adams, C.N. Bailey, S.R. Bandler, J.A. Chervenak, M.E. Eckart, F.M. Finkbeiner, R.L. Kelley, C.A. Kilbourne, F.S. Porter, J.E. Sadleir, *Journal of Low Temperature Physics*, Volume 167, Issue 3, pp 168175 (2012).
- [30] “Development of position-sensitive transition-edge sensor X-ray detectors”, S.J. Smith, S.R. Bandler, R.P. Brekosky, A.-D. Brown, J.A. Chervenak, M.E. Eckart, F.M. Finkbeiner, N. Iyomoto, R.L. Kelley, C.A. Kilbourne, F.S. Porter, J.E. Sadleir, E. -Feliciano, *IEEE Transactions on Applied Superconductivity* 19(3) (2009) 451-455.
- [31] “Development of arrays of position-sensitive microcalorimeters for Constellation-X” S.J. Smith, S.R. Bandler, R.P. Brekosky, A.-D. Brown, J.A. Chervenak, M.E. Eckart, E. Figueroa-Feliciano, F.M. Finkbeiner, R.L. Kelley, C.A. Kilbourne, F.S. Porter, J.E. Sadleir, *Proc. SPIE* 7011 (2008) 701126.
- [32] “Small-pixel position-sensitive microcalorimeters with four and nine absorbers attached”, S.J. Smith et al., in preparation (2016). Presented at LTD-15, HEAD-2013, ASC-2012, and SPIE-2012.
- [33] “Time-division superconducting quantum interference device multiplexer for transition-edge sensors”, P.A.J. de Korte, J. Beyer, S. Deiker, G.C. Hilton, K.D. Irwin, M. MacIntosh, S.W. Nam, C.D. Reintsema, L.R. Vale, M.E. Huber, *Rev. Sci. Instr.*, 74, 3807 (2003).
- [34] “Code-division multiplexing for x-ray microcalorimeters”, G. M. Stiehl, W. B. Doriese, J. W. Fowler, G. C. Hilton, K. D. Irwin C. D. Reintsema, D. R. Schmidt, D. S. Swetz, J. N. Ullom, L. R. Vale, *Appl. Phys. Lett.* 100, 072601 (2012).
- [35] “Demonstration of a multiplexer of dissipationless superconducting quantum interference devices”, J. A. B. Mates, G. C. Hilton, K. D. Irwin, K. W. Lehnert, L. R. Vale, *Appl. Phys. Lett.* 92, 023514, (2008).
- [36] “High resolution gamma-ray spectroscopy with a microwave multiplexed TES array”, O. Noroozian, J.A.B. Mates, D. Benne., J. Brevik, J. Fowler, J. Gao, G. Hilton, R. Horansky, K.D. Irwin, Z. Kang, D. Schmidt, L. Vale, J.N. Ullom, *Applied Physics Letters*, Vol 103, Issue 20, 202602 (2013)
- [37] “Developments in Time-Division Multiplexing of X-ray Transition-Edge Sensors”, W.B. Doriese, K.M. Morgan, D.A. Bennett, E.V. Denison, C.P. Fitzgerald, J. W. Fowler, J.D. Gard, J.P. Hays-Wehle, G.C.Hilton. K.D.Irwin, Y.I. Joe, J.A.B.Mates, G.C.ONeil, C.D. Reintsema, N.O. Robbins, D.R. Schmidt, D.S. Swetz, H. Tatsuno, L.R. Vale, J.N. Ullom, *J Low Temp Phys*, DOI 10.1007/s10909-015-1373-z, LTD-16 (2016).
- [38] “Review of superconducting transition-edge sensors for x-ray and gamma-ray spectroscopy”, J.N. Ullom, D.A. Bennet, *Supercond. Sci. Technol.* 28 084003 (2015).
- [39] “Optimising the multiplex factor of the frequency domain multiplexed readout of the TES-based microcalorimeter imaging array for the X-IFU instrument on the ATHENA x-ray observatory”, J. v.d. Kuur et al, these proceedings.
- [40] “Microwave SQUID Multiplexer for the Readout of Metallic Magnetic Calorimeters”, S.Kempf, L. Gastaldo, A. Fleischmann, C. Enss *J. Low. Temp. Phys.* 175 850-860 (2014).